CFD STUDY ON COOLANT MIXING IN VVER-440 FUEL ROD BUNDLES AND FUEL ASSEMBLY HEADS

S. Tóth, A. Aszódi

Budapest University of Technology and Economics, Institute of Nuclear Techniques
Műegyetem rkp. 9, 1111 Budapest, Hungary
Email: toth@reak.bme.hu, aszodi@reak.bme.hu

Abstract

A CFD model of VVER-440 fuel assembly heads was developed based on the technical documentation of a full-scale test facility built in the Kurchatov Institute, Moscow. Steady-state and transient calculations were performed to validate the model with a measurement set and investigate the effects of the spatial discretization, choosing of different turbulence models and use of different inlet boundary conditions. Inlet boundary conditions were determined both with COBRA subchannel code and with a fuel rod bundle CFD model that was built for this special purpose. The sensitivity studies showed that grid of about 8 million cells and BSL Reynolds Stress model are suitable to receive accurate prediction for the signal of the in-core thermocouples. The results were also compared against the experimental data. The results of the rod bundle calculations received with both subchannel and CFD codes differ significantly from the experimental data in some peripheral points. Whereas the results of the assembly head model are in relatively good agreement with the measured data. Best prediction for the signal of the in-core thermocouple was achieved with transient calculation using inlet boundary conditions generated by the CFD fuel rod bundle model. These calculations pointed out the difference between the outlet average temperature of the coolant and the temperature at the housing of the in-core thermocouple. Besides, the significant role of the outflow from the central tube was also proven. The transient runs revealed intensive coolant mixing with relatively large temperature fluctuations.

1. INTRODUCTION

In the VVER-440/213 type reactors (Russian designed PWR) the reactor core outlet temperature field is measured with in-core thermocouples installed above 210 fuel assemblies. These measured temperature values are fundamental information for the on-line core monitoring system. Based on these values, the radial distributions of the neutron flux and the assembly power are determined. Furthermore, these data have significant role in the limitation of the reactor power and in the prediction of the outlet temperatures of the fuel assemblies on positions without temperature measurements. For these purposes, it is desirable to process the temperature values measured by the thermocouples adequately. Originally, the measured values were supposed to be equal with the outlet average temperatures. In the last few years several CFD calculations called attention to the fact that this assumption is generally not acceptable (Toppila, 2004), (Légrádi, 2004), (Klučárová 2006) due to the imperfect coolant mixing in the fuel assembly heads. Naturally, these deviations have not caused any notable operational problems due to the use of conservative margins in the processing of the in-core temperature measurement data. However, the plans for applying new type of fuel assemblies (use of burnable poisons etc.) and the research activity around the technical conditions of power upgrade placed this question into the fore.

In order to perform experimental investigations, a test facility was built in the Kurchatov Institute (Russia) and extensive measurement series were carried out (Kobzar, 2006). The test facility included a full-scale model of a VVER-440 fuel assembly from the bottom level of the active part up to the head part. The heat generation in the fuel rods was reproduced with heating elements of different electric resistances. The heating elements were arranged in three groups, which could be fed from separate power supplies thus heat generation of higher non-uniformity could be modeled as well. The

temperature distributions were measured in 39 points at the outlet of the rod bundle and in 31 positions at the level of the in-core thermocouple. The measurements were performed under close-to-operational conditions (coolant pressure, temperature and mass flow, pin powers). Based on the technical documentation of the test facility, a VVER-440 fuel assembly head model was developed with the code ANSYS CFX (ANSYS, 2007) at our institute. A CFD model of the VVER-440 fuel pin bundles was built as well in order to determine inlet boundary conditions for the head model. An important goal was to validate these models with the experimental data measured in the Kurchatov Institute. Then, the validated models will be applied to specify a correction for the in-core temperature measurements. The above models, comprehensive sensitivity studies, the results of the calculations and their validations are described in the paper.

2. ROD BUNDLE CALCULATIONS

2.1 Description of the rod bundle model

The fuel assemblies of the VVER-440 type reactors consist of three main parts: assembly legs, rod bundles and assembly heads. Rod bundles include 126 fuel rods arranged in a triangular lattice, 11 spacer grids and a central tube for the self-powered neutron detectors (SPND). The bundles are surrounded by assembly shrouds, which prevent the coolant mixing between the fuel assemblies.

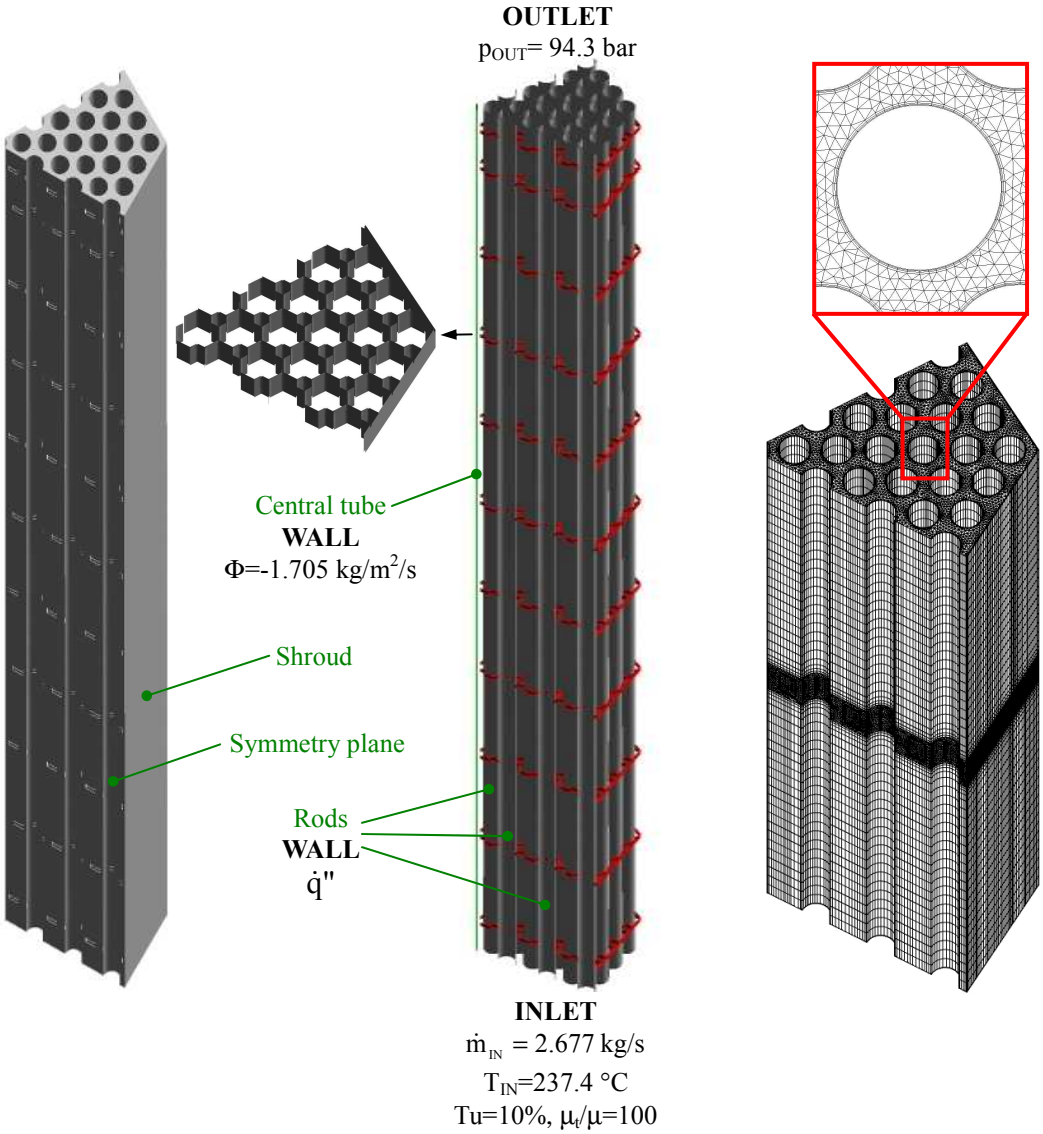

Fig. 1: Geometry, boundary conditions and mesh of the rod bundle model.

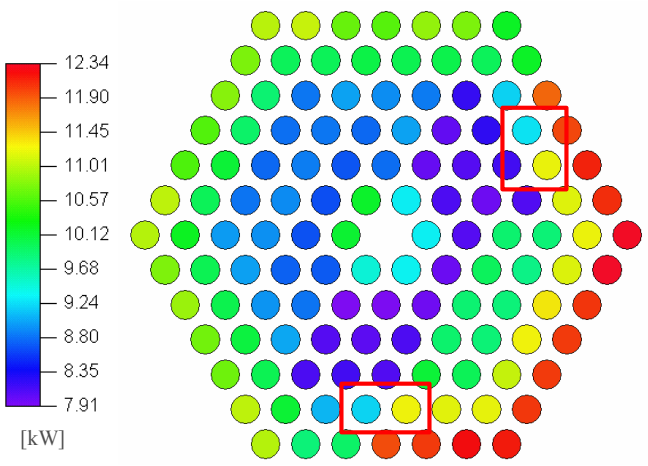

Fig. 2: Pin power distribution in the case of the measurement that was chosen for validation.

A CFD model of these pin bundles was developed for providing more realistic and accurate inlet boundary conditions for the assembly head model than a subchannel code can provide. A 60 degrees segment was modeled in order to limit the number of cells. By using this model inlet boundary condition sets for the assembly head model could be generated. The model includes the 2420 mm long active part and about 100 mm long inactive upper part of the rod bundles. 24 of the fuel pins, the central tube, the 11 spacer grids and the inner wall of the shroud were modeled (Fig. 1). The dimensions correspond to the dimensions of the model assembly that was investigated in the Russian experiment. Outer diameter of the rods is 9.1 mm and the rod pitch is 12.3 mm. Inner space of the shroud is 142.2 mm.

This complex model was built up from 11 submodels (see one of them on the right side in Fig. 1). Non-matching grids of neighbouring submodels were connected with GGIs (General Grid Interface). A subgeometry was meshed with a hybrid mesh consisting of tetrahedral, hexahedral and prismatic volume elements. Near the spacer grid, unstructured tetrahedral mesh was applied with prismatic layers close to the walls. Under and above the tetrahedral region extruded mesh of prismatic and hexahedral elements was used. The total number of the cells is about 9.5 million.

The parameters and boundary conditions of the model (Fig. 1) are based on the main conditions of the modeled experiment (Table 1). Inlet condition was given as coolant mass flow rate and temperature on the bottom surface of the model. Unfortunately, turbulence quantities were not measured during the experiment therefore the turbulence intensity and viscosity ratio are based on assumptions. No-slip smooth wall boundary condition with uniform heat flux was set on the surfaces of the rods. Heat flux values were calculated from pin powers determined in the experiment (Fig. 2). Outlet boundary condition was used with relative average pressure on the top surface. The reference pressure was 94.3 bar. On the side planes, symmetry constraints were used. Surfaces of the shroud, central tube and spacer grids were treated as adiabatic no-slip smooth walls. The inflow from the rod bundle into the central tube through its small cuts was modeled as a surface sink. The mass flux of the sink was determined based on measured data. BSL Reynolds Stress turbulence model with automatic wall treatment (ANSYS, 2007) was used in the calculations. BSL Reynolds Stress model is a second-order closure model in which transport equations for individual Reynolds stresses and for specific dissipation are solved. In an earlier work, it was justified that this model is suitable to calculate the characteristics of the flow field in VVER-440 rod bundles (Tóth, 2007).

High Resolution scheme (ANSYS, 2007) was applied as discretization scheme for the advection terms. This scheme uses a numerical correction to overcome the diffusive nature of the upwind scheme without introducing local oscillations. Temperature and pressure dependencies of the water coolant were taken into account using the IAPWS-IF97 data implemented in the code. Computations were performed in steady-state mode. Convergence criteria were 10^{-5} for the RMS of residuals and 0.01% for the imbalances.

Table 1: Main conditions of the chosen measurement.

Pressure at rod bundle exit [bar]	94.3
Inlet temperature of coolant [°C]	237.4
Total mass flow [t/h]	57.82
By-pass flow [t/h]	0
Total heat power [kW]	1,244.6
Heat power of group 1 [kW]	588.2
Heat power of group 2 [kW]	380.5
Heat power of group 3 [kW]	275.9
Outlet temperature of coolant from cenral tube [°C]	244.4

2.2 Results of the rod bundle calculations

Computations were performed for each 60 degrees segment of the rod bundle using six INTEL XEON 2000 and 3000 MHz processors for each calculation. Total computation time of the six calculations was about 120 hours. With this run-batch, the goal was determination of the inlet boundary condition for the assembly head model. Fig. 3 shows the temperature distributions at the end of the heated rod bundle – which corresponds to the inlet level of the assembly head model – calculated with the CFX code and COBRA subchannel code (Rowe, 1973). It can be seen that the characteristic of the results is similar and shows the characteristic of the pin power distribution. Naturally, the COBRA code gave subchannel average values therefore the temperature distribution is more uniform in that case.

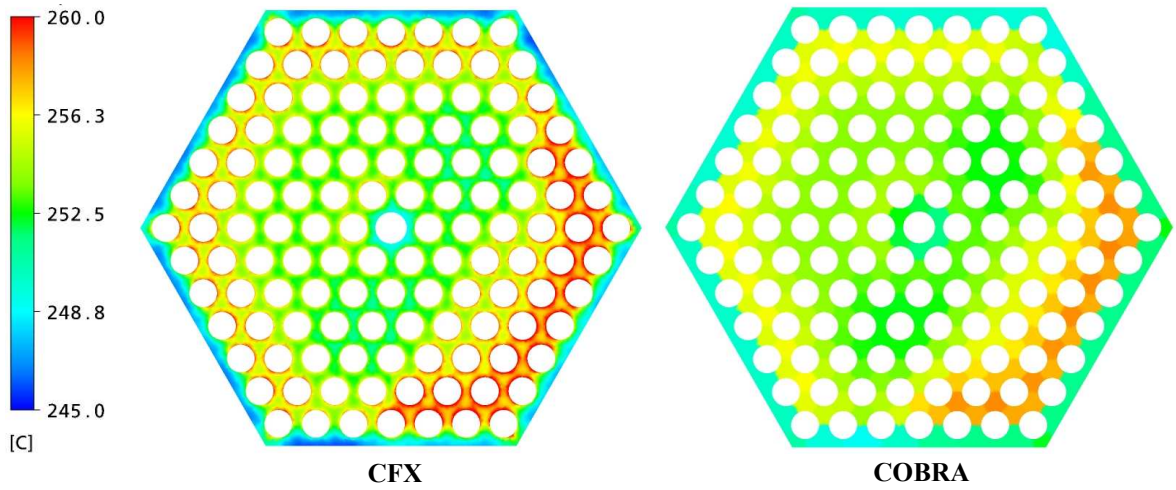

Fig. 3: Temperature distributions at the end of the heated rod bundle.

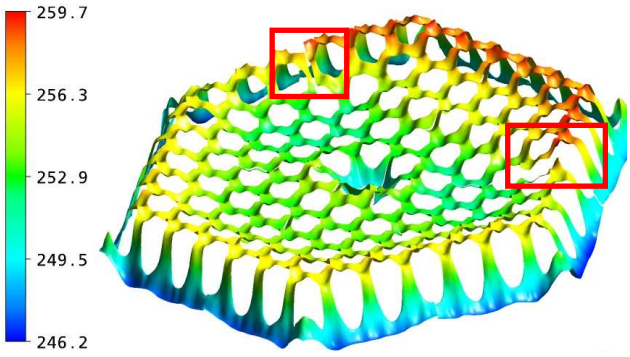

Fig. 4: Temperature surface at the outlet calculated with the CFX rod bundle model.

Fig. 4 shows the temperature surface at the rod bundle outlet. Near the adiabatic walls (shroud, central tube), the temperature gradient is quite larger than in the remaining region. There are two significant jumps in the temperature field (marked by red rectangles in Fig. 4). The origin of these jumps is the significant power deviations between neighbouring pins at the 60-degree symmetry planes. The problematic two pin pairs are marked by red rectangles in Fig. 2. These discrepancies could be eliminated with performing calculations with coupling two or more rod bundle segments.

Fig. 6 shows the temperature distributions along measuring radiuses (see Fig. 5) shifted with the outlet average temperature calculated from the heat balance. The measured values and the calculated ones with COBRA and CFX codes are presented also. In some points, measured values are missing because the corresponding data were not given. In most cases, the temperatures given by the COBRA code well correspond to subchannel average temperatures at the CFX calculation. It is important to note that the COBRA code generally gave 0.5-1.5 °C higher temperature results than the CFX code in the measuring points. The main reason is that the COBRA code determines subchannel average values while the CFX code can calculate spatial temperature distributions. The results point out that difference between these temperature values is usually not negligible therefore the measurement data can not be used directly for validating the COBRA model.

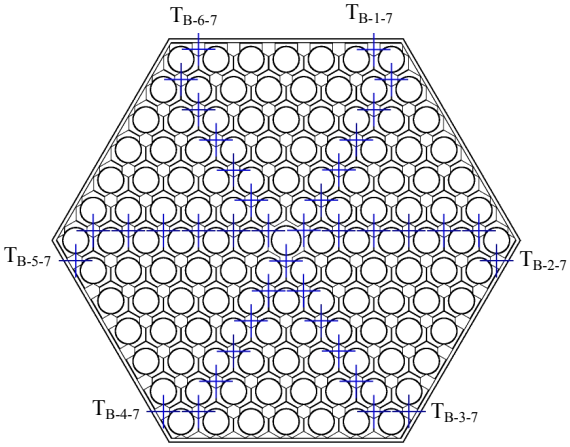

Fig. 5: Measuring points at the outlet of the rod bundle.

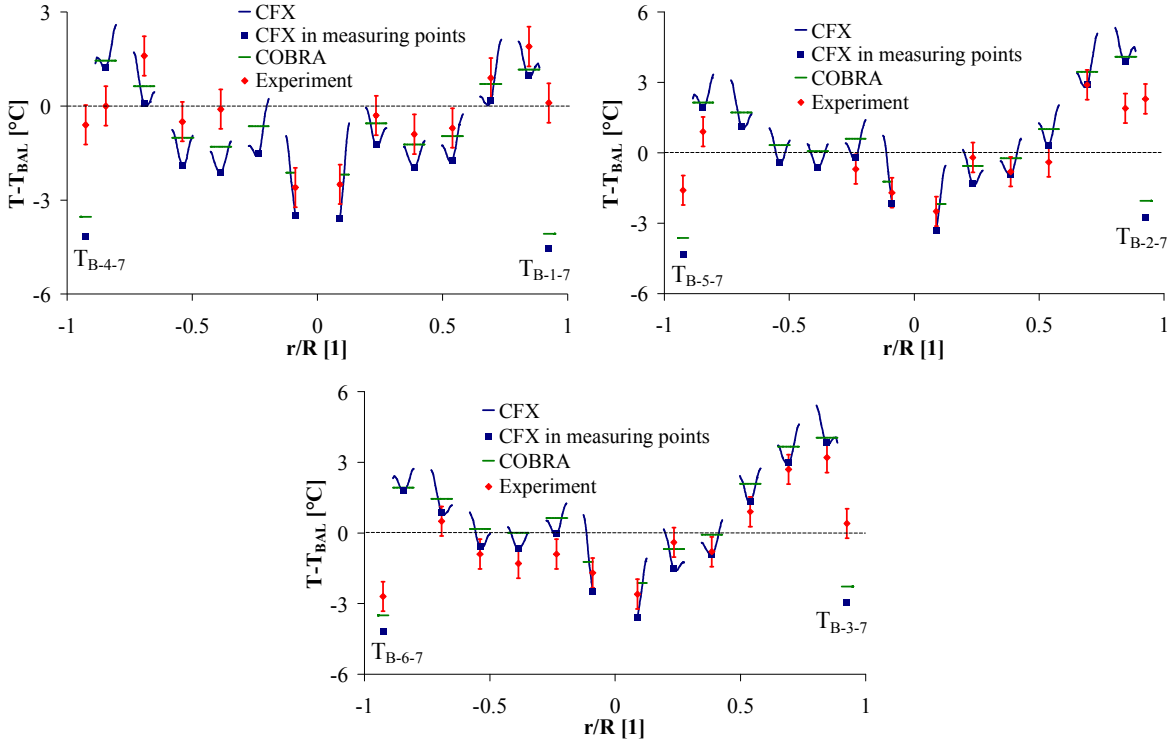

Fig. 6: Temperature distributions along radiuses at the outlet of the rod bundle.

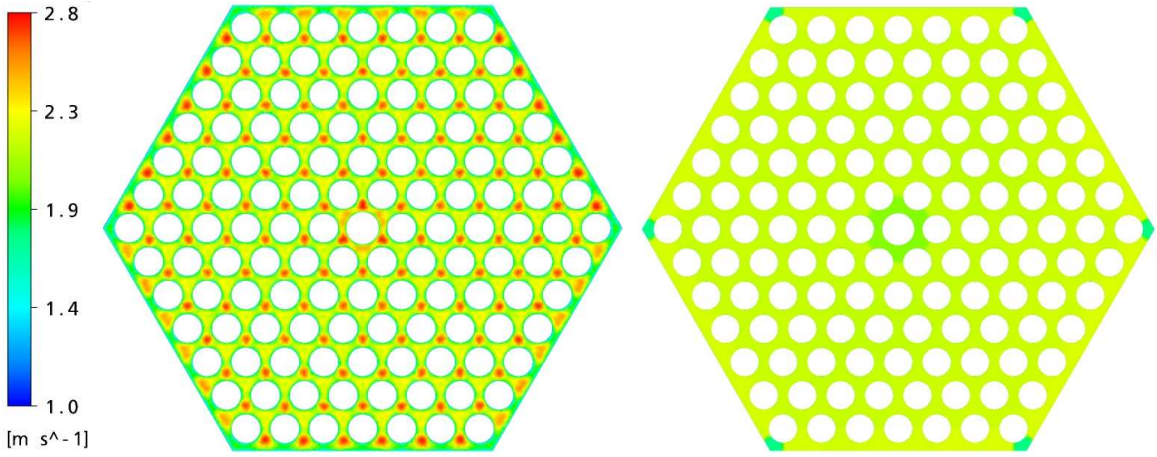

Fig. 7: Axial velocity distributions at the end of the heated rod bundle.

The characteristics of the deviations from the measurements are rather similar in spite of that fundamentally different computational approaches were used. Large differences of 3-4.5 °C can be experienced in the peripheral points. These deviations can not be explained only with the inaccuracy of the calculation. Exploration of possible reasons (e.g. inaccuracy in positioning of the thermocouples) is in progress. Less differences can be observed in the inner region.

Distributions of the axial velocity at the end of the heated rod bundle are shown in Fig. 7. In the case of the CFX result, impact of the spacer grid can be observed clearly. Naturally, COBRA code is not able to catch the effect of the grid in details therefore the velocity field calculated with it is much more homogeneous.

3. ASSEMBLY HEAD CALCULATIONS

3.1 Description of the assembly head model

The geometry model of VVER-440 assembly heads (Fig. 8) was built based on technical documentation of the test facility. The top level of the fuel rods' active part was chosen to be the bottom level of the model. Hereby the inlet was moved farther from the region of interest in order to ensure more realistic conditions. The outlet was defined at the upper core support plate, which is connected to the fuel assembly head from above and contains the in-core thermocouples. The model includes all parts of the assembly head which are important from the point of view of the coolant mixing.

Three different meshes were developed in order to examine the mesh sensitivity of the target variable, i.e. the average temperature on the thermocouple housing (marked by red in Fig. 8). Because of the complexity of the geometry hybrid meshes with the same structure were developed. The bottom region (Fig. 9/B) was meshed with tetrahedral elements near the spacer grid and with prism elements below and above the tetrahedral zone. Three flat mesh layers were developed near the walls to resolve better the strong gradients (Fig. 9/C). Owing to its irregular shape, the top region (Fig. 9/A) was meshed with also tetrahedral cells and with flat prisms in the near-wall region. Local grid refinements were applied in various parts of the geometry (at the ending of the pins, around the mixing grid, the catcher and thermocouple housing). Non-matching meshes of the bottom and top regions were connected with GGI interface. Since our goal was the investigation of the coolant mixing in assembly heads, the mesh resolution was changed in the top region only. The main characteristics and notations of the girds are shown in Table 2. Fine and coarse meshes were developed with refinement and coarsening of the base mesh. The effective grid refinement ratio (Eq. 1) was about 1.2.

$$r_{eff} = \left(\frac{N_1}{N_2} \right)^{1/D} \tag{1}$$

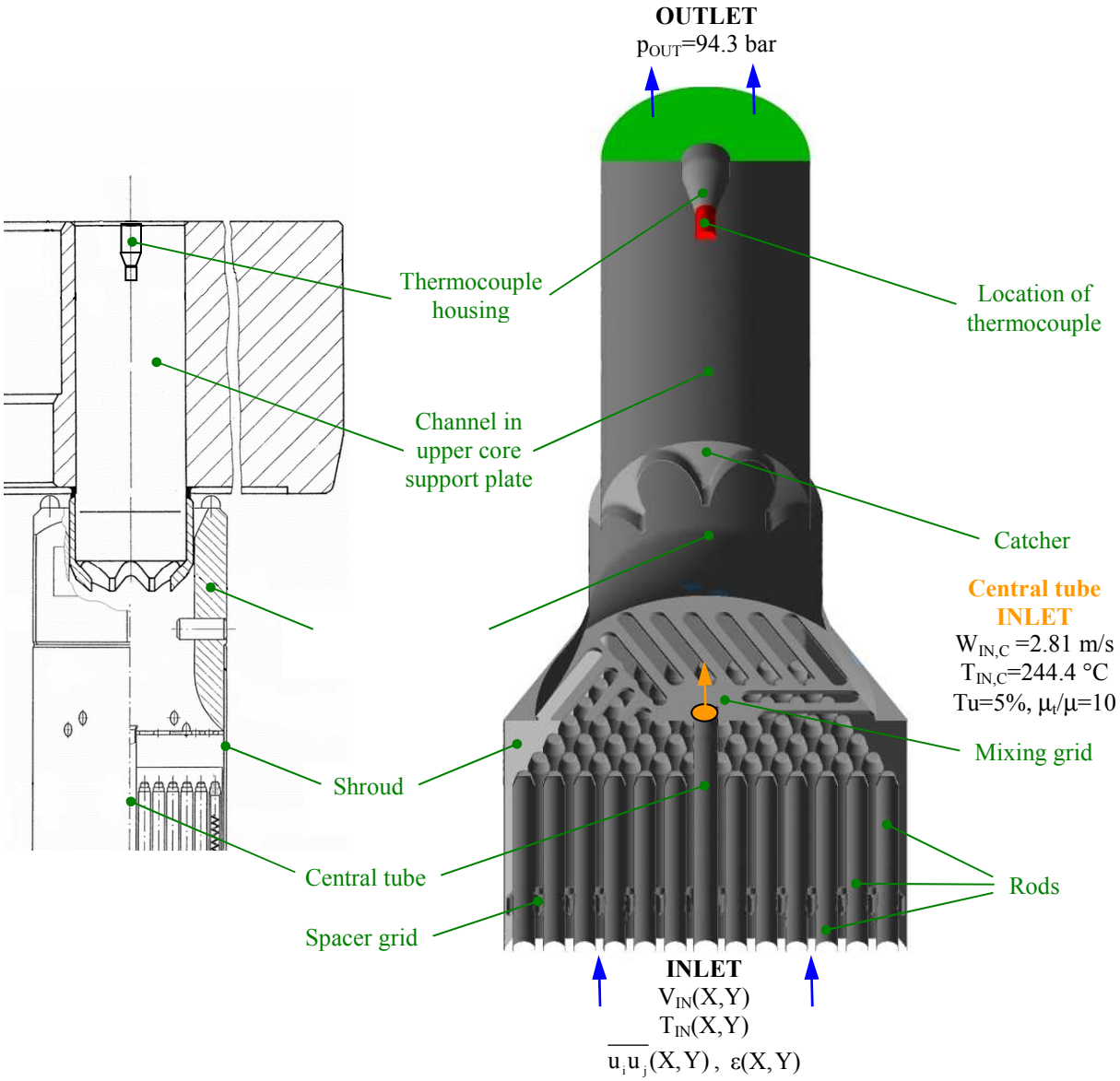

Fig. 8: Geometry and boundary conditions of the fuel assembly head model (cutaway view).

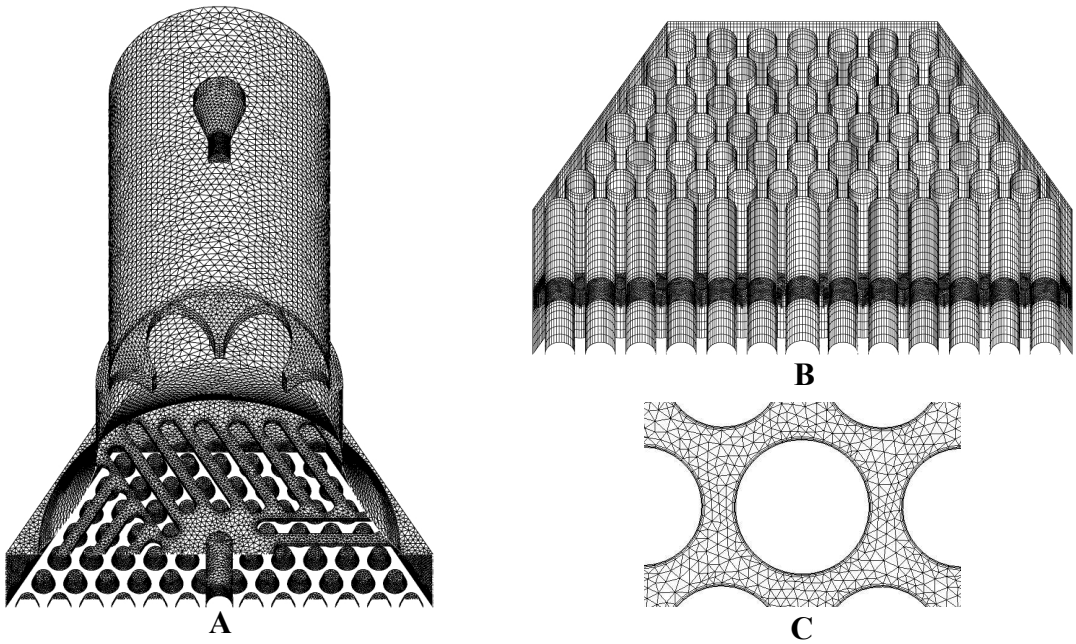

Fig. 9: Mesh of the fuel assembly head model (cutaway view).

Table 2: Main characteristics of the meshes

	Coarse mesh	Base mesh	Fine mesh
Scale factor	1.2	1	0.8
Total numer of cells	6,009,476	8,046,001	10,656,716
Number of cells in top part	1,946,198	3,982,723	6,593,438
Number of nodes in top part	501,655	911,945	1,470,522
Effective refinement ratio	-	1.22	1.17

Table 3: Main characteristics of the calculations

	Velocity boundary condition	Temperature boundary condition	Type of simulation
SVST_R	COBRA	COBRA	Steady state
CVCT_R	CFX	CFX	Steady state
SVST_UR	SVST_R	SVST_R	Unsteady
CVCT_UR	CVCT_R	CVCT_R	Unsteady

Boundary conditions are presented in Fig. 8. Inlet condition was applied at the bottom plane of the model. Inlet temperature and velocity distributions were determined by using of COBRA or CFX codes (Fig. 3 and Fig. 7). In the SVST cases the inlet temperature and axial velocity distributions were specified based on COBRA calculation (see Table 3). Due to the lack of any measured data, the inlet turbulence intensity and viscosity ratio were given based on assumptions. In the CVCT cases the inlet parameters (velocity, temperature and turbulence quantities) were determined with the CFX rod bundle model described in the previous section. In both cases inlet boundary condition was applied at the end of the central tube in order to take into account the flow from it. The velocity and temperature values were set on the basis of experimental data. For turbulence quantities supposed values were given. At the top plane of the model outlet condition was applied with relative average pressure. Reference pressure was 94.3 bar. All physical walls were treated as no-slip smooth adiabatic walls.

Turbulence was modeled with SST (Menter, 1993), BSL Reynolds Stress and SAS-SST (Menter, 2005) models and their impacts were studied. SST model belongs to the two equation turbulence models. Transport equations for the turbulence kinetic energy and specific dissipation are solved and the eddy viscosity is calculated based on these parameters. This model combines the advantages of the k-ε and k-ω models in such a way that it blends between them and it accounts for the transport of the turbulent shear stress to give more accurate prediction for separation. This model is extensively used for solving industrial flow problems. BSL Reynolds Stress model is a second-order closure model, in which transport equations for individual Reynolds stresses and for specific dissipation are solved. Similarly to the SST model, it combines the advantages of ε and ω based models using a blending function. This complex model was expected to describe the fundamental turbulent processes in assembly heads. SAS (Scale-Adaptive Simulation) is an improved URANS (Unsteady Reynolds Averaged Navier-Stokes) method. This method allows resolution of turbulent spectrum in unstable flow regimes owing to introduction of von Kármán length-scale into the turbulence scale equation (into the ω-equation in the case of the SAS-SST model). In stable flow regions, the model provides the solution of the RANS (Reynolds Averaged Navier-Stokes) equations. The model has similar functionality like the DES (Detached Eddy Simulation) but it is less mesh sensitive. This model is proposed for calculations of flows with unsteady detached regions. Such regions were expected to develop in fuel assembly heads (behind the fuel pins, the mixing grid and the catcher). Each model was used with automatic near-wall treatment.

High Resolution scheme was applied for the discretization of the advection terms. Temperature and pressure dependencies of the water properties were taken into account using IAPWS-IF97 water data, which are implemented in the CFX code. Convergence criteria were 10^{-4} for the RMS of residuals and 0.01% for the imbalances.

First, steady-state runs were performed. Since 0.1-0.5 °C temperature fluctuations were experienced in upper measuring points during the iteration of the steady-state calculations transient

simulations were also accomplished. Only the upper part of the model was investigated in the transient runs. The initial and inlet boundary conditions were determined from the results of the corresponding former RANS simulations. The velocity components, temperature field, turbulence quantities (Reynolds stresses and turbulent dissipation in the case of the BSL Reynolds Stress calculation, turbulent kinetic energy and turbulent dissipation in the cases of the SST and SAS-SST calculations) on the GGI interfaces of the RANS calculations were used as inlet conditions for the transients. Second Order Backward Euler scheme was used for the temporal discretization. 0.00125 s time step was used. 1 s long processes were investigated in the cases of the calculations performed with BSL Reynolds Stress and SST turbulence models and 2 s long transient was run with the SAS model. These simulation times were long enough to evaluate the time-averaged temperatures in the measurement points with an uncertainty of 0.1 °C. Other boundary conditions and settings were the same as in the steady-state calculations.

3.2 Results of the sensitivity studies

3.2.1 Mesh sensitivity study

Our general goal is to develop CFD models with which the in-core thermocouples' signal can be reproduced. Therefore, the surface average temperature on its housing was chosen to be the target variable. Three girds with different resolutions were created and calculations were performed with using the same boundary conditions in order to investigate the impact of the spatial discretization on the target variable. The inlet boundary conditions were determined with the CFX rod bundle model thus ensuring more realistic inlet conditions and minimizing the error coming from it. BSL Reynolds Stress turbulence model was applied to decrease the modeling error. As it will be shown in the next subsection, this model gave the best solution for the target variable. Only the time-averaged results of URANS simulations are presented. Fig. 10 shows temperature profiles at the level of the in-core thermocouple (see Fig. 13) calculated on three meshes.

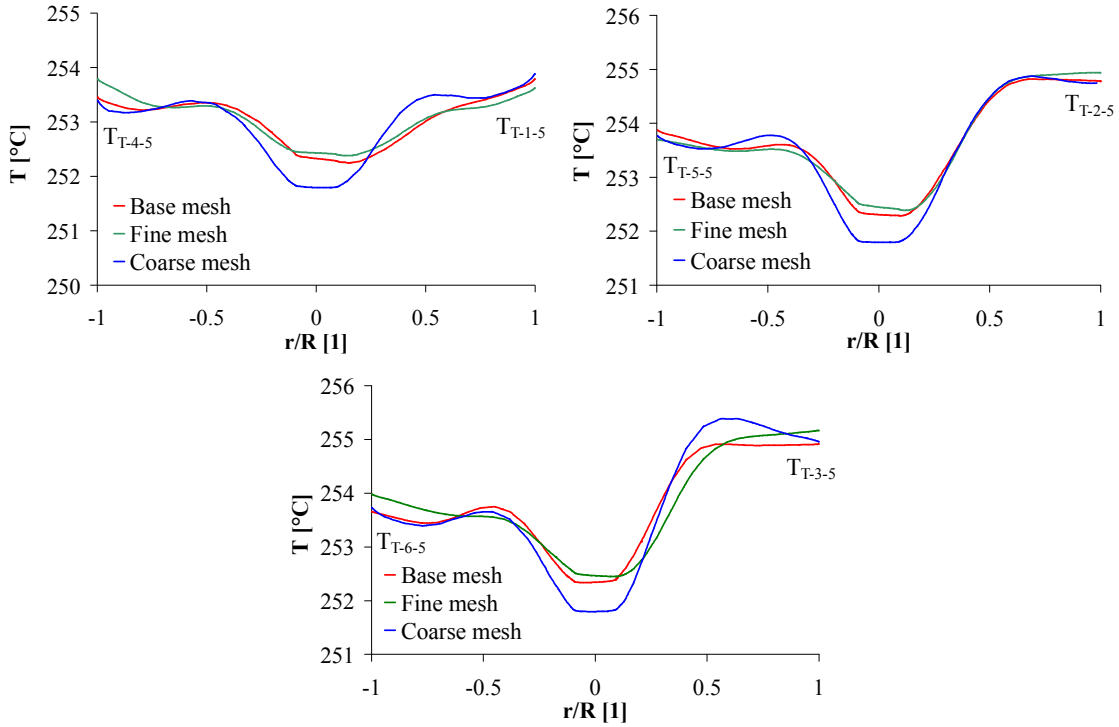

Fig. 10: Temperature profiles at the level of the in-core thermocouple calculated on the three girds.

Table 4: Main results of the mesh sensitivity study

Mesh	T_{OUT}	E_{TOUT}	T_{ST}	E_{TST}
	[°C]	[°C]	[°C]	[°C]
Coarse mesh	253.82	0.12	251.88	-0.72
Base mesh	253.81	0.11	252.39	-0.21
Fine mesh	253.81	0.11	252.48	-0.12
Experiment	253.8±0.63	0.10	252.6±0.63	-
Heat balance	253.7	-	-	-

These profiles show rather similar characteristic. The deviation between profiles calculated on the base and fine meshes is much smaller than it is between profiles calculated on the base and coarse meshes. By increasing the mesh density, the deviances are decreased and the results converge towards the mesh-independent solution.

The main results of the mesh sensitivity study are summarized in Table 4. Each calculated outlet average temperature values are in good agreement with the measured data. Difference between target variables computed on the base and fine meshes is negligible and both values agree well with the experimental data. By using coarse mesh, more inaccurate solution was obtained, which deviates stronger from other calculated values and measured data, therefore this gird was rejected.

The magnitude of spatial discretization errors can be assessed with the grid convergence index (GCI). In case the solutions on three grids were in the asymptotic region, the following expression should approach the order of the discretization scheme (Mahaffy, 2007):

$$p = ln\left(\frac{T_{ST,Coarse} - T_{ST,Base}}{T_{ST,Base} - T_{ST,Fine}}\right) / ln(r_{eff}) \tag{2}$$

The average value of the refinement ratios is 1.2; the calculated order of the convergence is about 9.5, which is clearly a non-physically value. Expected order of applied High Resolution scheme is between first-order and second-order (i.e. between 1 and 2). Possible reasons may be: the coarse mesh solution is not in the asymptotic region or the mesh refinement is not perfectly global and systematic. For this reason, an approximate value of 1.5 was considered for the convergence order. GCI is defined for the fine grid as follows:

$$GCI_{Fine} = F_s \left|\frac{T_{ST,Fine} - T_{ST,Base}}{T_{ST,Fine}}\right| \frac{1}{r_{eff}^{\ p} - 1} \tag{3}$$

GCI is defined for the coarser mesh as follows (Roache, 1997):

$$GCI_{Base} = F_s \left|\frac{T_{ST,Fine} - T_{ST,Base}}{T_{ST,Fine}}\right| \frac{r_{eff}^{\ p}}{r_{eff}^{\ p} - 1} \tag{4}$$

A value of 3 was used for the factor of safety because an approximate value was considered for the order of the grid convergence. GCI for the fine mesh solution is about 0.4% and 0.5% for the base mesh solution, which values are acceptable.

Whereas perfect mesh-independent solution was not reached, the temperature profiles calculated on the base and fine meshes do not differ considerably and target values agree with the measured data well. Therefore, both grids were valued as acceptable. For the further calculations, the base mesh was chosen because of its smaller computational effort needs.

3.2.2 Sensitivity study on the turbulence model

The sensitivity study on the turbulence model was carried out with use of the SST, SAS-SST and BSL Reynolds Stress turbulence models. During this study, the base mesh was used and inlet boundary conditions determined with CFD code were applied. The time-averaged temperature profiles at the in-core thermocouple level are shown in Fig 11. Profiles differ from each other but the sensitivity on turbulence model can not be said strong. The main time-averaged results of the calculations are given in Table 5. Outlet average temperatures do not differ from each other. The target variable calculated with SST model is farthest from the measured value. SAS-SST simulation provided a more accurate prediction than the URANS SST calculation and it corresponds satisfactorily with the experimental data. This improvement comes from the use of the SAS method, which allows a more adequate simulation of turbulent structures in detached flow regions than the URANS method do. BSL Reynolds Stress model provided the best result for the target variable, which corresponds well with the experimental data. This is a consequence of higher description level of turbulence in comparison to the SST model. Therefore, BSL Reynolds Stress model was selected for further calculations.

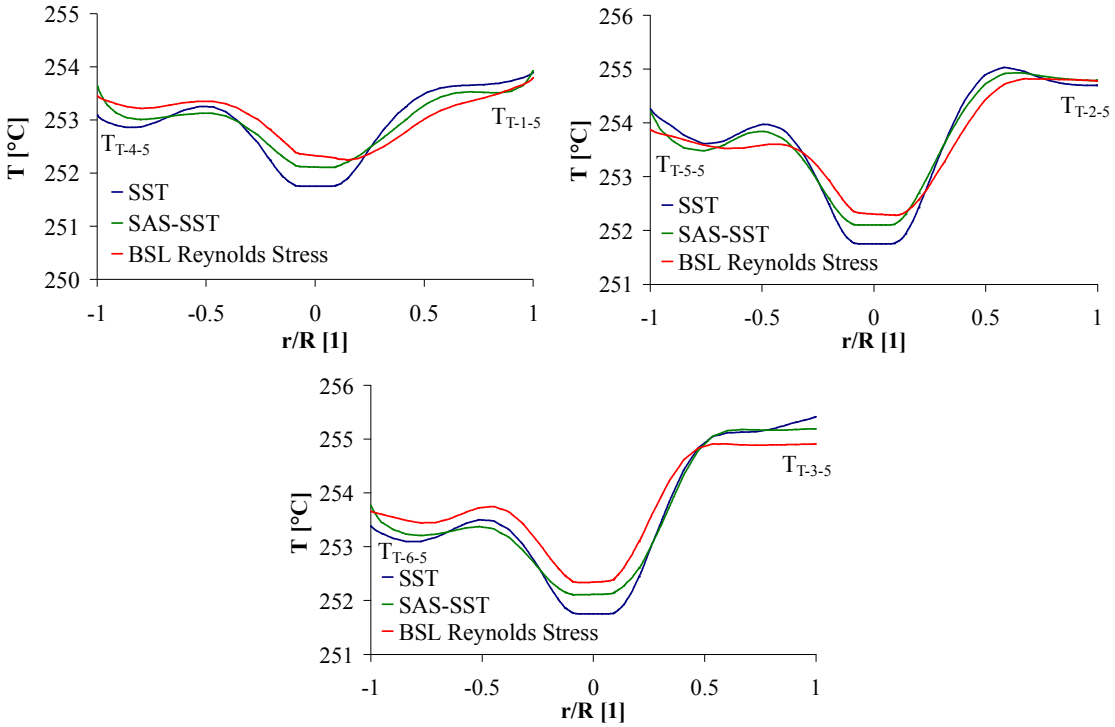

Fig. 11: Temperature profiles at the level of the in-core thermocouple calculated with the three turbulence models.

Table 5: Main results of mesh sensitivity study

Turbulence model	T_{OUT} [°C]	E_{TOUT} [°C]	T_{ST} [°C]	E_{TST} [°C]
SST	253.80	0.10	251.82	-0.78
SAS-SST	253.80	0.10	252.19	-0.41
BSL Reynolds Stress	253.81	0.11	252.39	-0.21
Experiment	253.8±0.63	0.10	252.6±0.63	-
Heat balance	253.7	-	-	-

3.3 Results of the assembly head calculations

With base mesh and BSL Reynolds Stress turbulence model, calculations were performed. Several inlet boundary condition sets were used that were determined with COBRA subchannel code or CFD rod bundle model. Simulations were run on four INTEL XEON 3000 MHz processors. A steady-state simulation needed about 16 hours while approximately 95 hours were necessary for a transient calculation. Since qualitative differences were not experienced between the results, only SVST_R run is presented in details.

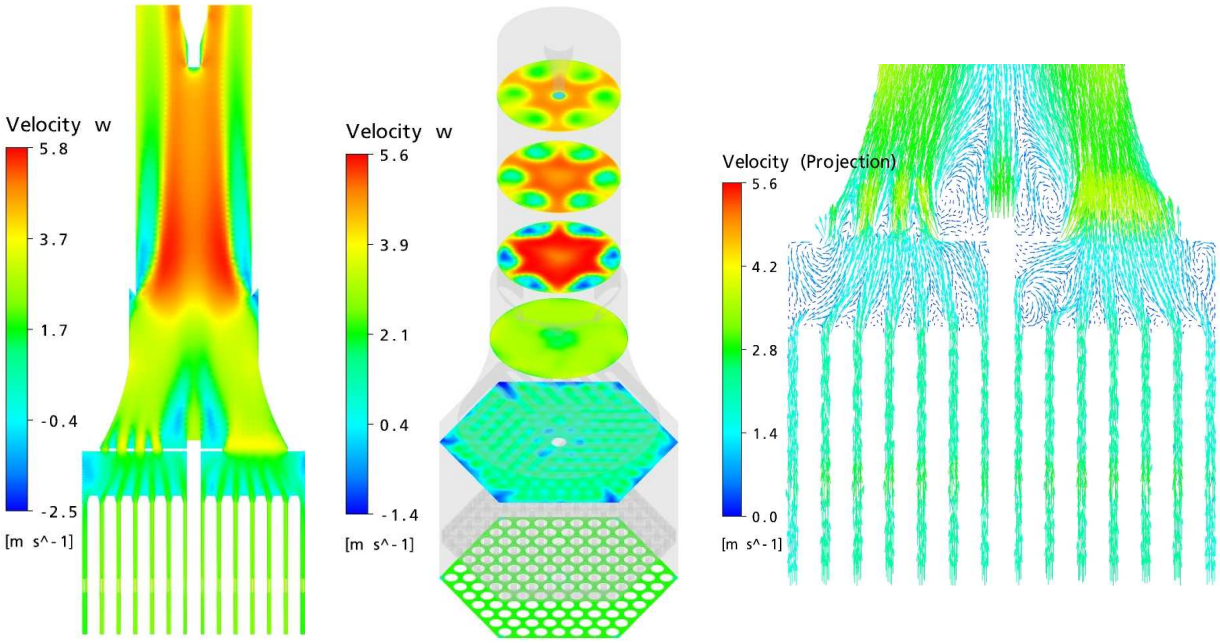

Fig. 12: Velocity field in the assembly head (SVST_R calculation).

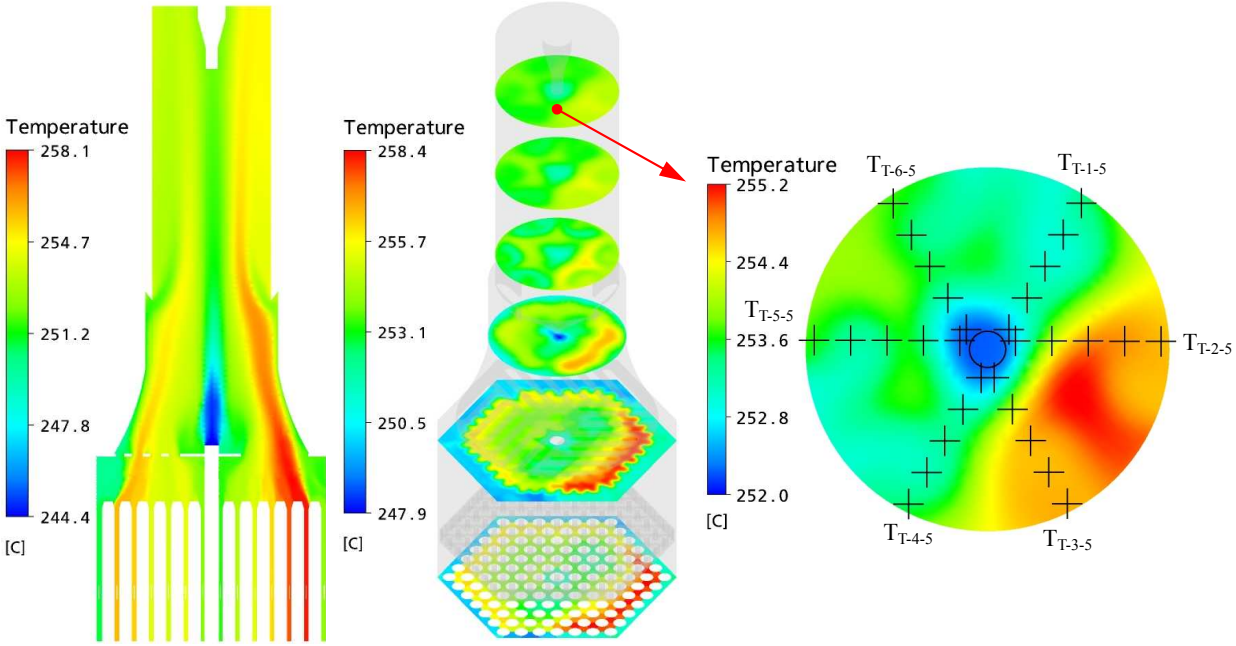

Fig. 13: Temperature field in the assembly head (SVST_R calculation).

Fig. 12 represents the velocity field in the assembly head. The velocity field is relatively uniform among the fuel rods. Above the rods, eddies develop in many locations (behind the pins, in the corners between the shroud and the mixing grid) and these eddies intensify the coolant mixing. In the holes of the mixing grid, the velocity increases and further swirls form behind it. The largest eddies evolve near the centre of the mixing grid. Approaching the catcher, the velocity distribution becomes relatively uniform. Behind it, the velocity increases in the middle region and additional eddies develop in the peripheral zone. The trace of the catcher can be observed clearly at the level of the in-core thermocouple.

Fig. 13 shows the temperature field. At the inlet, the temperature distribution is inhomogeneous and this characteristic practically does not change along unheated part of the rod bundle. Above the rods, intensive mixing can be observed due to the contribution of the large eddies. Moving down-stream, the temperature field becomes more homogeneous because of the effects of the mixing grid and catcher, but the mixing is not perfect to the in-core thermocouple. The main characteristics of the inlet temperature distribution can be discovered in the peripheral zone at the level of the thermocouple. Around the thermocouple housing, the temperature is lower due to the lower temperature outflow from the central tube. Thus, the in-core thermocouple measures a significantly lower value than the outlet average temperature in the investigated case. Based on these results, modeling of the outflow from the central tube is not negligible because it has an important impact on the temperature measurements.

In Fig. 14, the temperature fluctuations in some points can be seen in the case of the CVCT_UR simulation. Large fluctuations (0.8-1.8 °C) can be observed close to the housing of the in-core thermocouple. The magnitude of the fluctuations is smaller farther from the middle region.

Fig. 15 shows the temperature profiles (shifted with the outlet average temperature calculated from the heat balance) along radiuses at the level of the in-core thermocouple (Fig. 13). In the cases of the URANS calculations the time-averaged values are given. It can be seen that there are no significant differences between the results of the unsteady and steady calculations by the same boundary conditions. It must be mentioned that the uncertainties of the URANS results are smaller due to use of adequate time-averaging. SVST and CVCT results do not differ essentially despite differences in the inlet boundary conditions.

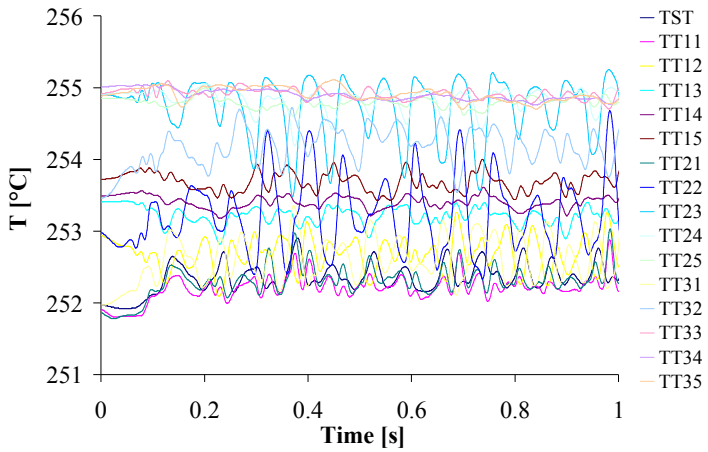

Fig. 14: Temperature fluctuations in some points (CVCT_UR calculation).

Good agreement can be experienced between the measured data and simulation results in spite of the large deviations in the inlet boundary conditions. Generally, close to the thermocouple housing the temperature values are slightly underestimated while in the outer region they are slightly overestimated.

The main results of the calculations and measurement are summarized in Table 6. The calculated outlet average temperatures of the coolant correspond well with the measured data and with the value that was calculated from the heat balance. Every simulation gave an acceptable prediction for the average temperature on the thermocouple housing. The result of the CVCT_UR calculation (transient simulation, inlet boundary condition determined with CFX code) agrees the best with the measured value.

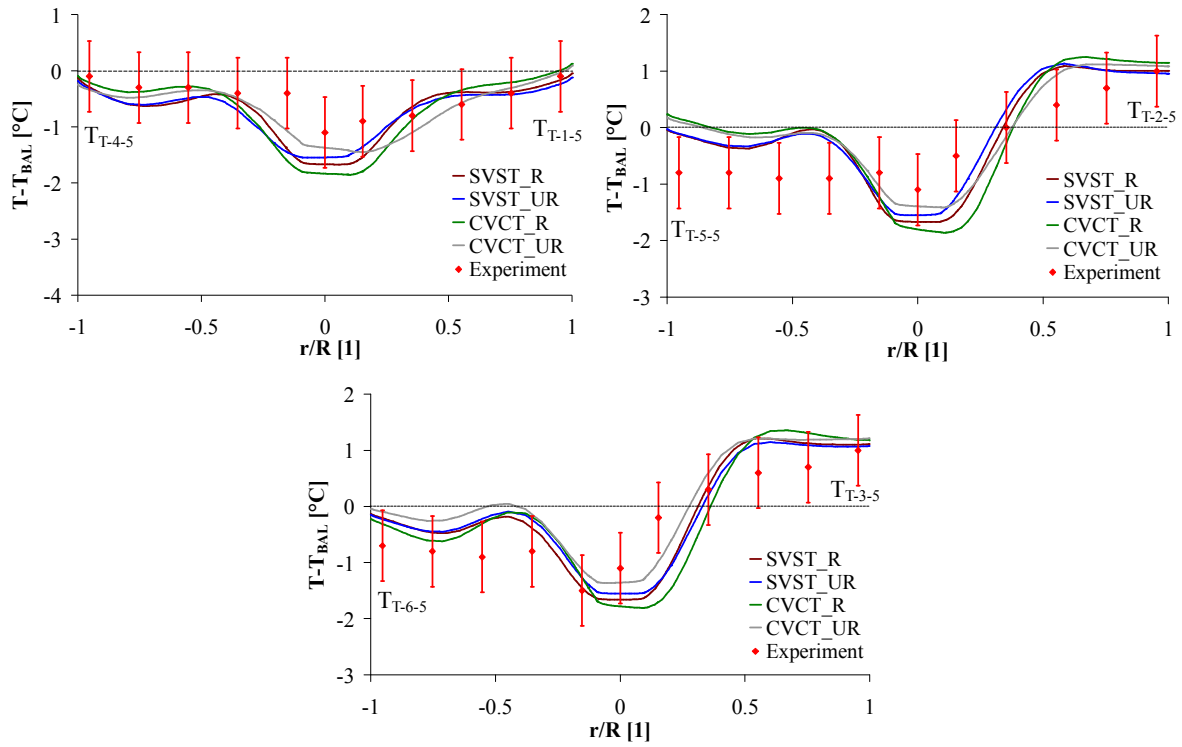

Fig. 15: Temperature profiles along radiuses at the level of the in-core thermocouple.

Table 6: Main numerical results of the assembly head calculations

	T_{OUT}	E_{TOUT}	T_{ST}	E_{TST}	ΔT_{ST}	δT_{ST}
	[°C]	[°C]	[°C]	[°C]	[°C]	
SVST_R	253,74	0,04	252,11	-0,49	-1,59	-9,8%
CVCT_R	253,79	0,09	251,97	-0,63	-1,73	-10,6%
SVST_UR	253,74	0,04	252,22	-0,38	-1,48	-9,1%
CVCT_UR	253,81	0,11	252,39	-0,21	-1,31	-8,0%
Experiment	253.8±0.63	0,10	252.6±0.63	-	-1,1	-6,7%
Heat balance	253,7	-	-	-	-	-

4. CONCLUSIONS

A detailed CFD model of the head part of VVER-440 fuel assemblies was developed based on the technical documentation of a full-scale test facility that was built in the Kurchatov Institute, Moscow. Several calculations were performed for a measurement set. Validation of the model and investigation of sensitivity for the spatial discretization, turbulence model and inlet boundary condition sets were also performed. Inlet conditions were determined with both the COBRA subchannel code and a CFX rod bundle model that was developed for this special purpose. Comparison against experimental data is also shown.

The results of the COBRA subchannel code and the CFD rod bundle model are related to the experimental data similarly in spite of the fact that the codes are based on different fundamentals. The reasons of higher experienced deviations from the measured data in peripheral points are being investigated. The CFD calculations showed that the experimental data can not be used directly for validating the COBRA model.

The mesh sensitivity study for the assembly head model pointed out that using a grid of about 8 million cells reliable results can be achieved. The sensitivity study on the turbulence model showed that the simulation performed with the SAS-SST model gave better prediction for the target variable

than the calculation with the URANS SST model. The best results were obtained with URANS BSL Reynolds Stress model.

The simulations proved that the coolant mixing is more intensive in the fuel assembly head than in the rod bundle, but it is not perfect. Therefore, the in-core thermocouple generally measures a value that differs from the outlet average temperature of the coolant. The investigations showed that the outflow from the central tube influences strongly the temperature measurement therefore this flow has to be taken into account in VVER-440 assembly head calculations. The results of the fuel assembly head calculations are in relatively good agreement with the measurement data. Significant differences were not found between the results of the simulations performed by using inlet boundary conditions generated with the CFX or COBRA calculations. It seems that the assembly head model is less sensitive to the quality of the inlet boundary sets thus acceptable results can be achieved using inlet condition sets calculated with the COBRA subchannel code. The transient simulations predicted unsteady flow with large temperature fluctuations near the housing of the in-core thermocouple. By using the same boundary condition sets, steady-state and transient simulations gave close to the same results for the time-averaged temperature values. Anyway, the application of transient calculations is more suitable from the point of view of the reduction of calculation uncertainties. Best prediction for "in-core temperature measurement" was achieved with transient calculation using inlet boundary conditions generated by the CFX fuel rod bundle model.

In the near future, examination of additional measurement sets is aimed in order to strengthen the validation of the model. The validated assembly head model will be applied in the determination of a correction for the in-core thermocouple signals.

ACKNOWLEDGMENTS

Authors express their thanks to the colleagues working at Reactor Physics Department of Nuclear Power Plant Paks for providing the COBRA calculations and for the transmission of experimental results of the Kurchatov Institute.

NOMENCLATURE

D	dimension of the problem
E_{TOUT}	T_{OUT}-T_{BAL}, where T_{BAL} is the outlet average temperature of the coolant calculated from the heat balance
E_{TST}	T_{ST}-T_{ST_M}, where T_{ST_M} is the temperature measured with regular thermocouple
F_s	factor of safety
$\dot{m}_{IN}$	inlet mass flow rate
N_i	number of grid points
r_{eff}	effective gird refinement ratio
p	rate of the grid convergence
p_{OUT}	outlet pressure
$\dot{q}''$	wall heat flux
$T_{B\text{-}X\text{-}X}$	temperatures at the outlet of the rod bundle
T_{IN}	inlet temperature
T_{OUT}	outlet average temperature of the coolant
T_{ST}	average temperature on the in-core thermocouple housing (Fig.2 marked by red)
$T_{T\text{-}X\text{-}X}$	temperatures at the level of the regular thermocouple
Tu	turbulence intensity
v_{IN}	inlet velocity
ΔT_{ST}	T_{ST}-T_{BAL}
δT_{ST}	$\Delta T_{ST}/\Delta T_{BAL}$, where ΔT_{BAL} is warm up of the coolant calculated from the heat balance
Φ	mass flux
μ	dynamic viscosity
μ_t	turbulent dynamic viscosity

REFERENCES

ANSYS Inc., "ANSYS CFX-Solver Modeling Guide", "ANSYS CFX-Solver Theory Guide" (2007).

K. Klučárová, J. Remiš, "The CFD Modeling of Coolant Flow in Fuel Assembly - Current Results and Their Application", *Proc. 16th Symposium of AER*, Bratislava, Slovakia, pp. 493-502 (2006).

L.L. Kobzar, D. A. Oleksyuk, "Experiments on Simulation of Coolant Mixing in Fuel Assembly Head and Core Exit Channel of VVER-440 Reactor", *Proc. 16th Symposium of AER*, Bratislava, Slovakia, pp. 95-117 (2006).

G. Légrádi, A. Aszódi, "Further Results on the Coolant Mixing in Fuel Assembly Head", *Proc. 14th Symposium of AER*, Helsinki, Finland, pp. 557-565 (2004).

J. Mahaffy et al., "Best Practice Guidelines for the Use of CFD in Nuclear Reactor Safety Applications", NEA/CSNI/R(2007)5, (2007).

F.R. Menter, "Two-equation eddy-viscosity turbulence models for engineering applications", *Proc. 24th Fluid Dynamics Conference*, Orlando, Florida, USA, AIAA-1993-2906 (1993).

F.R. Menter, Y. Egorov, "A Scale-Adaptive Simulation Model using Two-Equation Models", *Proc. 43rd AIAA Aerospace Sciences Meeting and Exhibit*, Reno, Nevada, USA, AIAA-2005-1095 (2005).

P. J. Roache, "Quantification of Uncertainty in Computational Fluid Dynamics", *Annu. Rev. Fluid. Mech.,* 29, pp. 123-160 (1997).

D.S. Rowe, "COBRA-IIIC: a Digital Computer Program for Steady-State and Transient Thermal Hydraulic Analysis of Rod Bundle Nuclear Fuel Elements", *Battelle Pacific Northwest Laboratory*, Richland, Washington, USA, BNWL-1695 (1973).

Zs. Szécsényi, B. Beliczai, Personal communication from Paks NPP, Paks, Hungary (2007).

T. Toppila, V. Lestinen, P. Siltanen, "CFD Simulation of Coolant Mixing Inside the Fuel Assembly Top Nozzle and Core Exit Channel of a VVER-440 Reactor", *Proc. 14th Symposium of AER*, Helsinki, Finland, pp. 567-579 (2004).

S. Tóth, A. Aszódi, "CFD Analysis of Flow Field in a Triangular Rod Bundle", *Proc. 12th International Topical Meeting on Nuclear Reactor Thermal Hydraulics*, Pittsburgh, Pennsylvania, USA, NURETH-12-175 (2007).